Journal of Applied Polymer Science

Morphology Study of Immiscible Polymer Blends in a Vane Extruder

Jin-Ping Qu,[1,2] Hui-Zhuo Chen,[1,2] Shu-Rong Liu,[1,2] Bin Tan,[1,2] Li-Ming Liu,[1,2] Xiao-Chun Yin,[1,2] Quan-Jin Liu,[1,2] Rui-Biao Guo[1,2]

[1]National Engineering Research Center of Novel Equipment for Polymer Processing, South China University of Technology, Guangzhou 510641, China

[2]Key Laboratory of Polymer Processing Engineering of Ministry of Education, South China University of Technology, Guangzhou 510641, China

Correspondence to: J.-P. Qu (E-mail: jpqu@scut.edu.cn.)

ABSTRACT: This study reports the morphology development of polymer blends in a novel vane extruder in which polymer mainly suffers from elongational deformation field. Rapidly cooled samples of polypropylene/polystyrene (PP/PS) are collected in the vane extruder after stable extrusion. Furthermore, the shape and size of the dispersed phase from initial to final stages are analyzed. In addition, in order to compare the final size of the dispersed phase, different immiscible blends, including polypropylene/polyamide and PP/PS, are prepared by vane extruder and twin-screw extruder, respectively. The results show that the dispersed phase is made to change rapidly from stretched striations to droplets under the strong elongational deformation field in the vane extruder. Furthermore, the droplet size of dispersed phase of blends prepared by vane extruder is much smaller than that prepared by twin-screw extruder, indicating that the vane extruder is more efficient in mixing for immiscible polymer blends. © 2012 Wiley Periodicals, Inc. J. Appl. Polym. Sci. 128: 3576–3585, 2013

KEYWORDS: morphology; blends; extrusion

Received 7 May 2012; accepted 7 September 2012; published online 28 September 2012
DOI: 10.1002/app.38573

INTRODUCTION

In recent years, to obtain advanced materials, polymer blending is becoming more and more effective. As compared to a new monomers or polymerization routes developing, it is less time-consuming, more environmental friendly and economical. Because of the great potential and advantages, the polymer blending has been attracting more and more attention.[1,2] However, the properties of the polymer blends barely meet the expectation for the incompatibility of the polymers. It is known that morphology development during processing is one of the critical factors to determine the performance of immiscible polymer blends. Regarding the morphology development, several literatures have been reported.[3–8] For single-screw extruder, the morphology development of difference stages has been studied.[9,10] Lindt and Ghosh[11] investigated the morphology development of polymer blends in a single-screw extruder, and found out the formation of fine lamellar structures during the early stages of morphology development. Tyagi and Ghosh[12] studied the evolution of morphology in single-screw extruder, which was from initial (presence of striation) stage to final (droplet formation) stage, and captured the breakup process at the start of compression zone, where both shear and elongational flow was applied. Moreover, the effects of material characteristics in single-screw extruder on morphology development are also reported. Huang et al.[13] investigated the influence of viscosity ratios on morphology development along the single-screw extruder and observed that morphological changes occurred during the initial softening stage of blending when the viscosity ratio is small. In addition, the morphology development in twin-screw extruder has also been published on several literatures.[14,15] Utracki and coworkers[16–19] reviewed the theoretical and experimental data on the breakup of droplets in twin-screw extruder, and proposed two different dispersion mechanisms. Bourry and Favis[20] studied three different PS/HDPE blends, which were fed via different procedures processing in a twin-screw extruder. The research showed that the final blend morphology of blends is predominantly determined by the melt state. Besides, morphology development of the immiscible polymer blends in chaotic mixing device was also studied besides in screw extruder.[21,22]

Considerable evidence has been accumulated to demonstrate that type of flow is an important factor on morphology development and final particle size of polymer. And shear flow and elongational flow are the two major types of flow in polymer processing. It is widely recognized that elongational flow in polymer processing has many advantages.[23] Elongational flow

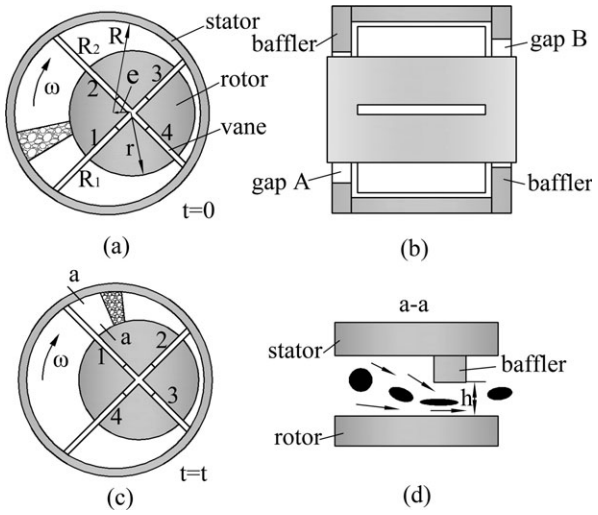

Figure 1. Schematic drawing of vane plasticizing and conveying unit (VPCU).

generates exponential stretching, while simple shear flow just gives linear stretching, which results that the dispersed phase droplets of blends are broken more efficiently in elongational flow than in shear flow.[15,24,25] Moreover, compared to shear deformation field, elongational deformation field consumes less energy to generate the same deformation of polymer.[26] Unfortunately, most of the polymer blends are prepared by polymer processing equipment of which the flow is mainly dominated by shear deformation field. Several efforts have been made to generate elongational flow field.[27,28] Bouquey et al.[29] built a laboratory-scale mixing device in which the flow was characterized by a high contribution from elongational flow, and observed that the materials dispersed better in the new device than the classical rotational batch mixer. Novais et al.[30] compared two melt mixing methods, which could generate flow with different characteristics. They observed that the converging/diverging flow sequence showed better performance on dispersion as compared with the twin-screw extruder. In recently, in order to generate considerable elongational flow field during polymer processing, Qu et al.[31,32] designed a novel polymer processing equipment known as vane extruder of which continuous dynamical converging channels[33] can generate strong elongational deformation field in the whole process.

In this study, the morphology development of immiscible blends in vane extruder is specifically investigated. Additionally, the morphologies and size of dispersed phase of immiscible polymer blends prepared by vane extruder and twin-screw extruder were also compared, respectively.

EXPERIMENTAL

Materials

Polypropylene [PP N-2306, MFI 12.5 g/10 min (270°C, 2.16 kg)] and polystyrene [PS N-236, MFI 40.2 g/10 min (270°C, 2.16 kg)] are supplied by China Petroleum and Chemical Polyamide [PA 103HSL, MFI 59.3 g/10 min (270°C, 2.16 kg)] is supplied by American Dupont.

Introduction of Vane Extruder

A self-developed vane extruder was employed in this article. Both the structure and processing principle of vane extruder are quite different from traditional screw extruder. It is comprised of several vane plasticizing and conveying units (VPCUs), as shown in Figure 1. Each VPCU is consisted of a stator, a rotor placed in the vertical direction of stator eccentrically, four vanes settled in the radial rectangle section of rotor, and two pieces of baffler with discharging gap. The stator, rotor, two vanes, and bafflers form a closed cavity, of which volume periodically changes from small to large and then back to small when the rotor rotates. Polymeric materials are fed into VPCU through gap A on one baffler when the closed cavity volume becoming larger and then discharged through gap B on another baffler when the closed cavity volume becoming smaller. In this way, polymeric materials are forwardly conveyed from one VPCU to another. It is noted that dynamical elongational deformation field (DEDF) is generated by the dynamical converging channels in VPCU, and the strength of the DEDF is controlled by converging ratio.[34] The converging ratio in VPCU can be calculated according to the following equations:[33]

$$\lambda_c = \frac{R_1 - r}{R_2 - r} = \frac{e\cos(\omega t) + \sqrt{R^2 - e^2\sin^2(\omega t)} - r}{e\cos(\frac{\pi}{2} + \omega t) + \sqrt{R^2 - e^2\sin^2(\frac{\pi}{2} + \omega t)} - r} \quad (1)$$

$$\lambda_a = \frac{R_1 - r}{h} = \frac{e\cos(\omega t) + \sqrt{R^2 - e^2\sin^2(\omega t)} - r}{h} \quad (2)$$

where λ_c and λ_a are the converging ratio in circumferential, respectively and discharging direction, R_1 and R_2 is the dynamical radius of vane 1 and vane 2, R and r are the inner radius of stator and outer radius of rotor, respectively, e is the eccentricity distance of the stator, t is time, ω is the angular velocity, and h is height of discharging gap.

Figure 2 is the schematic structure of a vane extruder. The vane extruder used in this article is consisted of 12 VPCUs. The inner diameter of the stator is 46 mm, the outer diameter of the rotor is 40 mm, and eccentricity distance between the rotor and stator is 3 mm.

Blends Preparation

All the materials (PP, PA, and PS) were dried at 80°C for 8 h in an oven before used. Before extrusion, the dried pellets at predetermined compositions and weight ratio were premixed in a high speed mixer machine. Subsequently, premixed blends were fed into the vane extruder. Then, the extruded strand taken from the end of the extruder die was immediately quenched in a water bath and dried. As comparison, a series of blends were

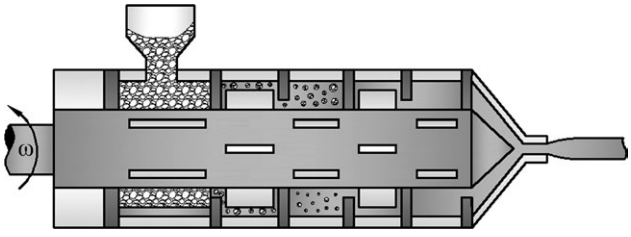

Figure 2. Schematic structure of vane extruder.

Table I. Composition of Blends and Processing Condition

Blends	Composition (wt %)	Processing temperature (°C)	
		Vane extruder	Twin-screw extruder
PP/PS	70/30	170-190-200-210-200	170-190-190-200-200-210-210-200
PP/PA	10/90-90/10	265-270-270-270-265	265-270-270-270-270-270-270-265

also prepared by a Brabender corotating twin-screw extruder (Φ = 25 mm, L/D = 40, DSE 20/40D Lab-Station, Germany) with the same die. In this study, the rotating speed of rotor in vane extruder and screw in twin-screw extruder was maintained at 30 rpm. The blends compositions and the temperature profiles from hopper to die of vane extruder and twin-screw extruder were given in Table I.

In addition, the blend PP/PS (70/30) was selected to investigate the morphology development in the vane extruder. The rotating speed of rotor in vane extruder was also set at 30 rpm. Once a steady extrusion state was reached, the vane extruder was abruptly stopped, and chilled at the same time with circulating cold water. Subsequently, cooled blends were taken from each VPCU of the vane extruder.

Phase Morphology Characterization

A scanning electron microscopy (SEM) (Qaunta 200, FEI, USA), operating at a 20 kV accelerating voltage, was used to observe the blend morphology. Cryofractured surfaces of different direction of blend in a VPCU were studied. Figure 3 shows the observed direction. θ is the circumferential direction of the rotor and Z is the axial direction of the rotor (discharge direction). To investigate the phase morphology more conveniently, series of cryofractured surfaces were etched with toluene reagent at 40°C for 8 h to remove the PS phase. The SEM micrographs of the cryofractured surfaces were analyzed to determine average particle size. An average of 500–1000 particles per sample was examined.

RESULTS AND DISCUSSION

The Morphology Development in the Vane Extruder

Figure 4(a) displays the PP/PS blends taken from the first VPCU of the vane extruder. It can be seen that a thin melt film formed near the surface of the stator and some of the pellets are deformed and squashed seriously. As shown in Figure 4(b, c), the solid pellets are deformed more seriously and the "solid bed" begins to break up in the second and third VPCU. At the same time, the melting zone gets larger which surrounds the "solid bed." As the solid state is majority in the two VPCUs, such a coexistence of both solid and melt state can be called solid-rich suspension. In the fourth VPCU, it can be directly observed that the majority of solid pellets are melted, just leaving a few solid pellets surrounded by melt [Figure 4(d)]. Such state can be named melt-rich suspension. And then all the solid pellets display melted phenomenon in the fifth VPCU, as shown in Figure 4(e, f).

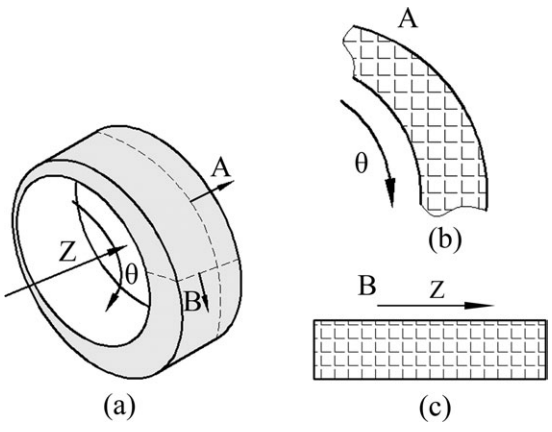

Figure 3. (a) Schematic of sample. (b) The cross-section along θ direction. (c) The cross-section along Z direction.

To characterize the morphology development in the vane extruder, SEM micrographs of PP/PS blend samples are studied [Figures 5–8]. Figure 5 shows the morphology of PP/PS blends in the sixth VPCU. It is observed in Figure 5(a) that PS dispersed in PP matrix appears striation structure and large droplet structure along θ direction. The average striation thickness is 13.09 μm, and the average diameter of large droplets beside the striation is 5.86 μm. The fact indicates that PS phase disperses nonuniform in PP matrix. Moreover, PS phase shows lamellar structure along Z direction [Figure 5(b)]. The cross-section shape of the lamellar structure displays ellipse, and its average long diameter is 4.78 μm, which reveals that the PS phase is elongated in both θ and Z direction.

The morphology of the PP/PS blends in the seventh VPCU is shown in Figure 6(a). It is clear that not only striation structure, but also different size droplet structures of PS dispersed phase coexist in the cross-section along θ direction. As compared with the sixth VPCU, the striation thickness and droplet size of PS phase in the seventh VPCU decreased significantly. Figure 6(b) displays that PS phase disperses uniformly in PP matrix and appears as droplet structure of average diameter of 2.07 μm in cross-section along θ direction in the eighth VPCU. Furthermore, PS phase appears as both lamellar and droplet structure in the cross-section along Z direction [Figure 6(c)], which indicates that the PP/PS blend suffers from elongational deformation seriously along the axial (Z) direction in the vane extruder, and some of PS dispersed phase are stretched into droplets.

Figure 7(a) shows the cross-section of PP/PS blend along θ direction in the ninth VPCU. It is interesting to note that compared with the eighth VPCU, the droplet size in the ninth VPCU becomes a little larger, and the average diameter is 2.98 μm. In addition, Figure 7(b) presents the transformation of PS phase from lamellar to droplet structure. Moreover, Figure 8(a–c) show the cross-section of PP/PS blend along θ direction in the 10th,

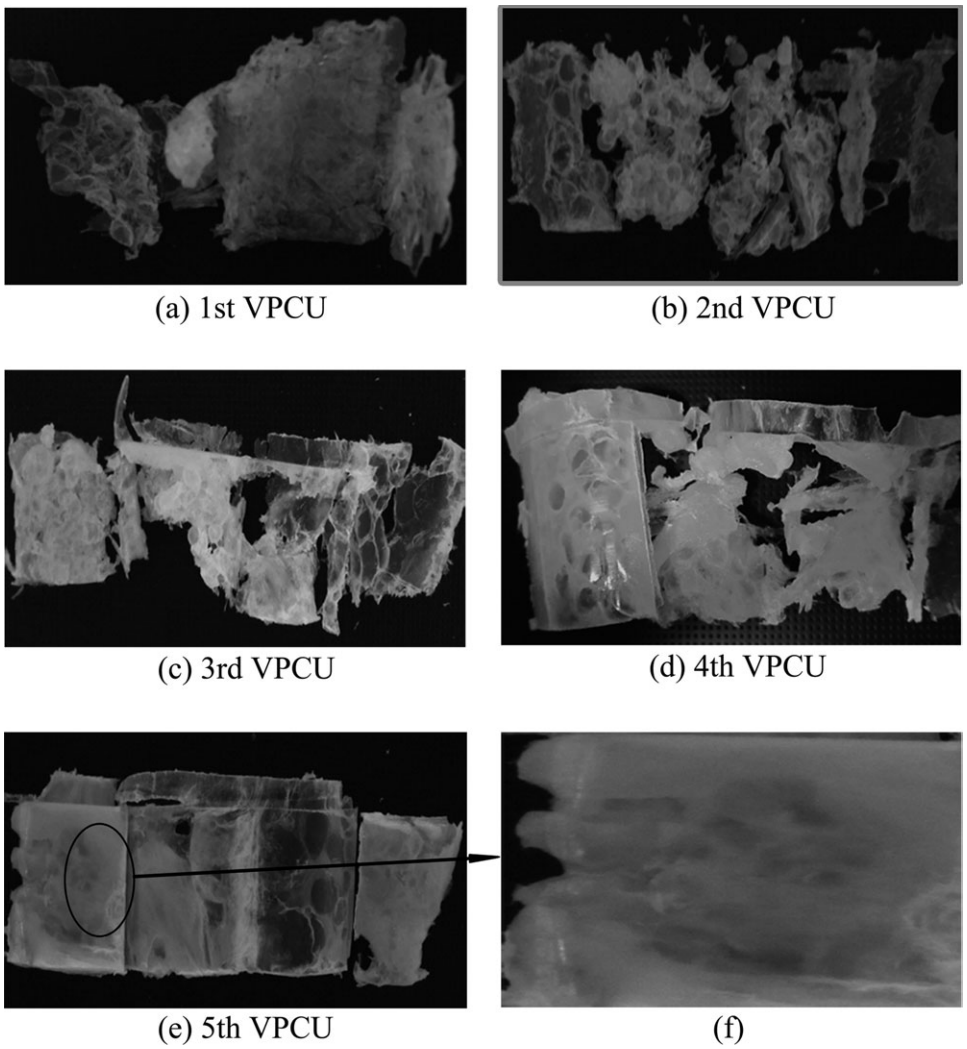

Figure 4. Photographs of PP/PS blend in first five VPCU.

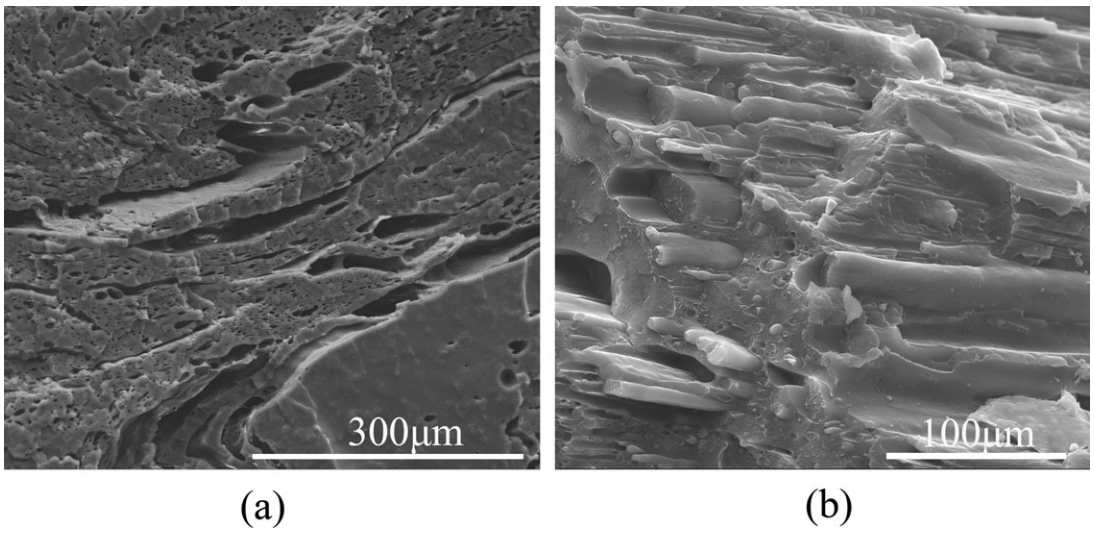

Figure 5. Morphology of PP/PS blend in the sixth VPCU. (a) The cross-section along θ direction (PS was etched). (b) The cross-section along Z direction.

Applied Polymer SCIENCE

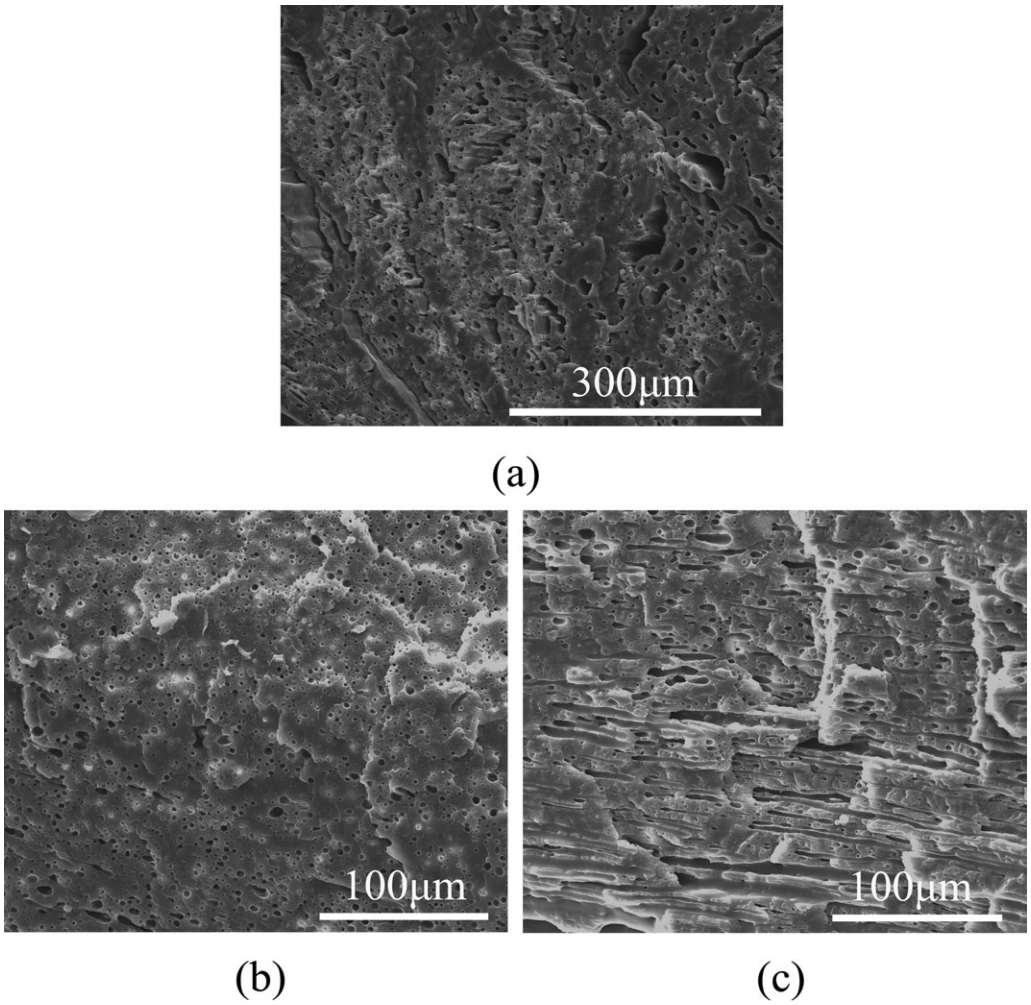

Figure 6. Morphology of PP/PS blends (PS was etched). (a) The cross-section along θ direction in the seventh VPCU. (b) The cross-section along θ direction in the eighth VPCU. (c) The cross-section along Z direction in the eighth VPCU.

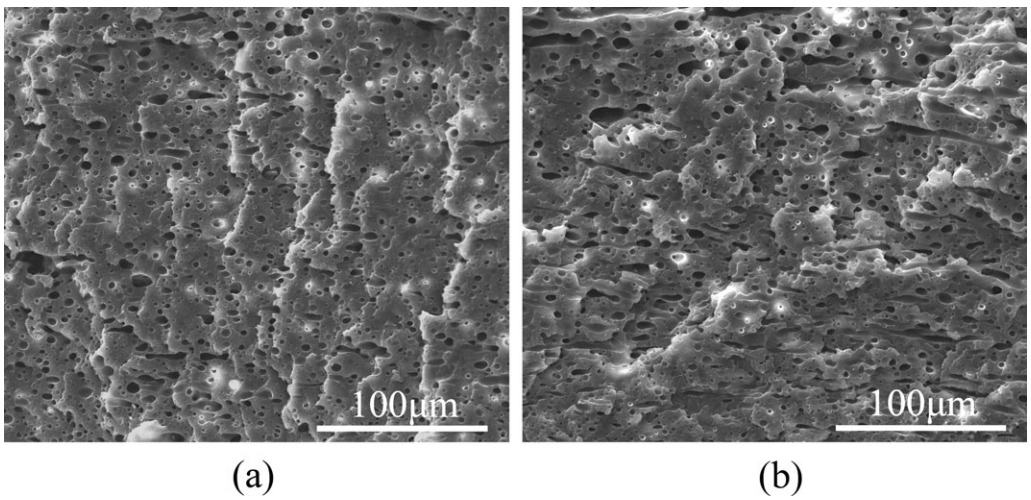

Figure 7. Morphology of PP/PS blend in the ninth VPCU (PS was etched). (a) The cross-section along θ direction. (b) The cross-section along Z direction.

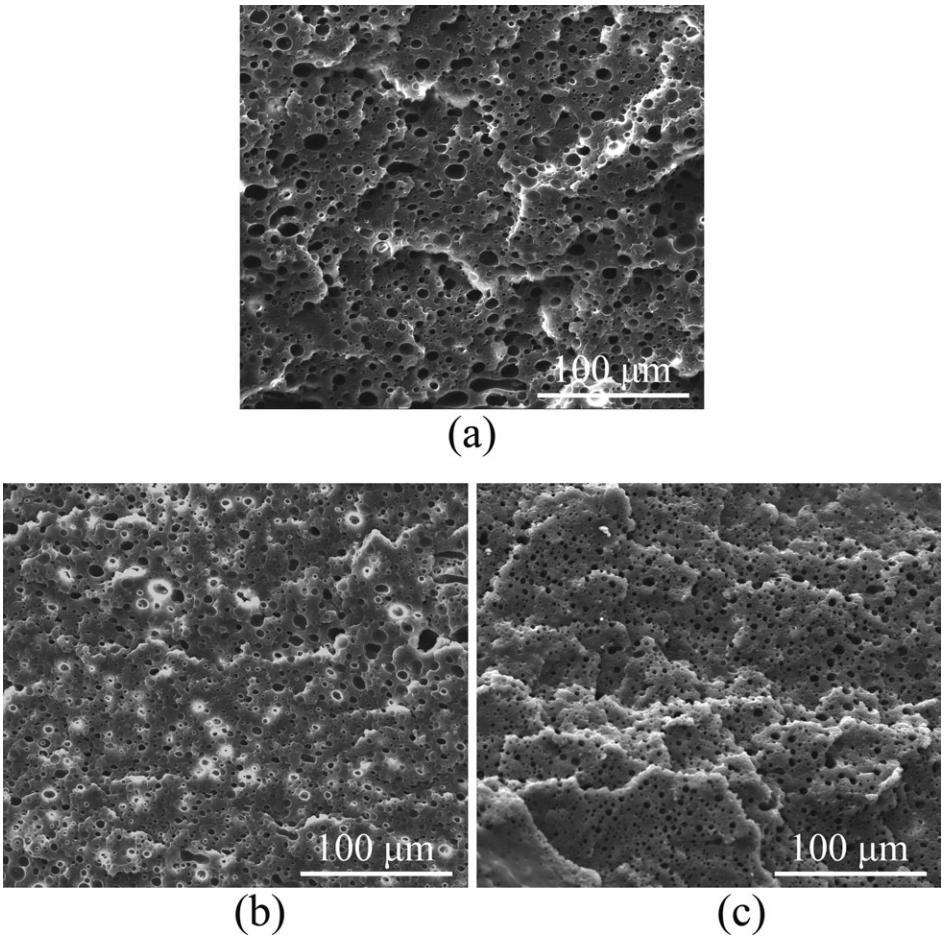

Figure 8. Morphology of PP/PS blends (PS was etched). (a) The cross-section along θ direction in the tenth VPCU. (b) The cross-section along θ direction in the eleventh VPCU. (c) The cross-section along θ direction in the twelfth VPCU.

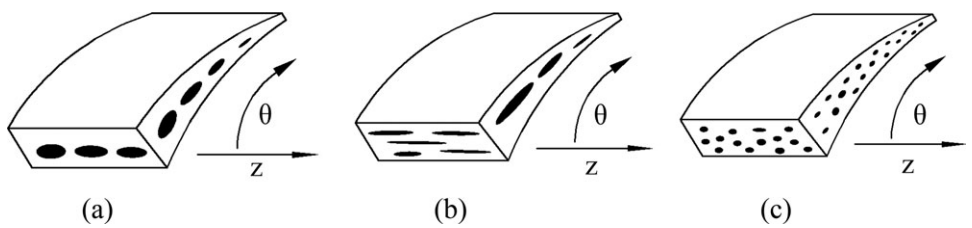

Figure 9. Schematic of morphology development along the length of vane extruder. (a) Stage of large particle. (b) Stage of droplet elongation. (c) Stage of droplet breakup.

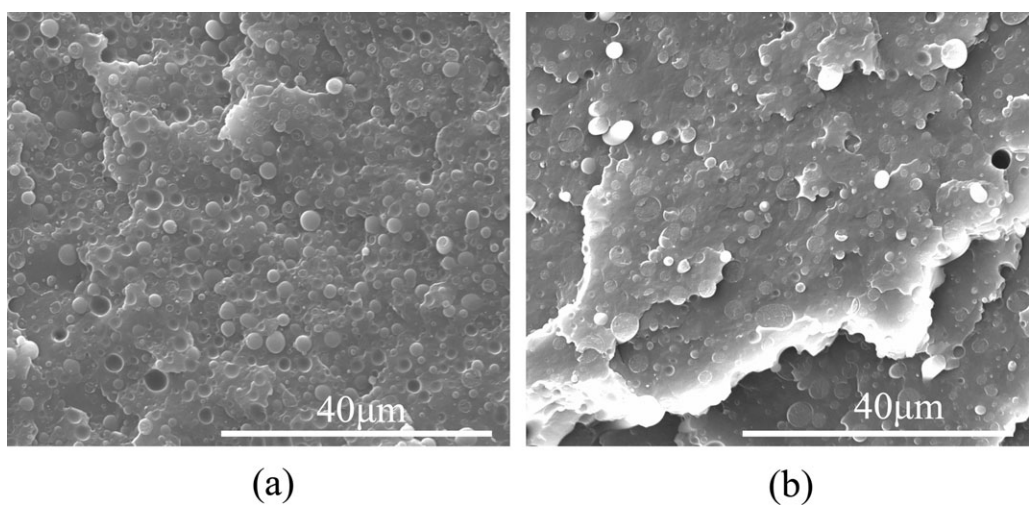

Figure 10. Morphology of PP/PS blends (vertical to flow direction). (a) Prepared by vane extruder. (b) Prepared by twin-screw extruder.

Applied Polymer SCIENCE

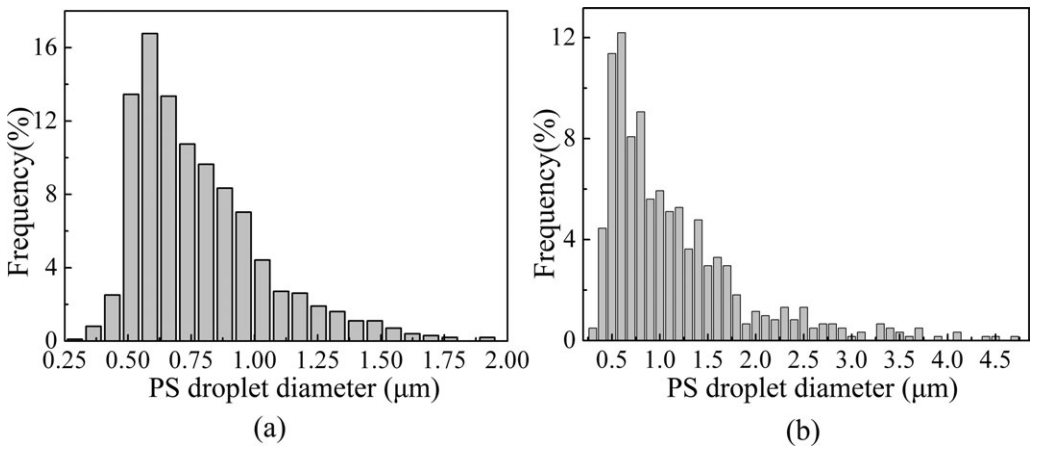

Figure 11. The droplet size distribution of dispersed phase in PP/PS blends. (a) Prepared by vane extruder. (b) Prepared by twin-screw extruder.

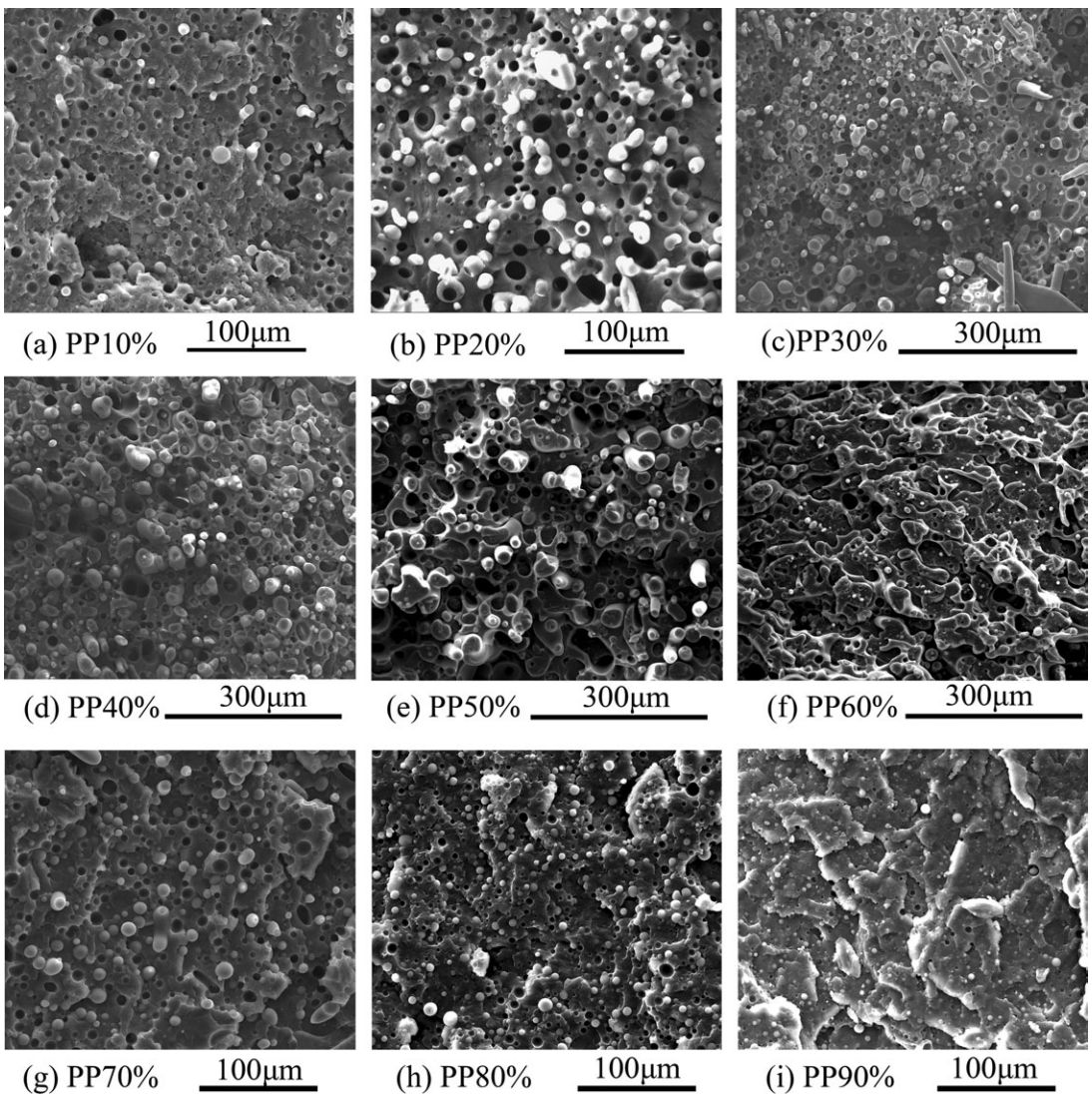

Figure 12. Morphology of PP/PA blends prepared by vane extruder (vertical to the extrusion direction).

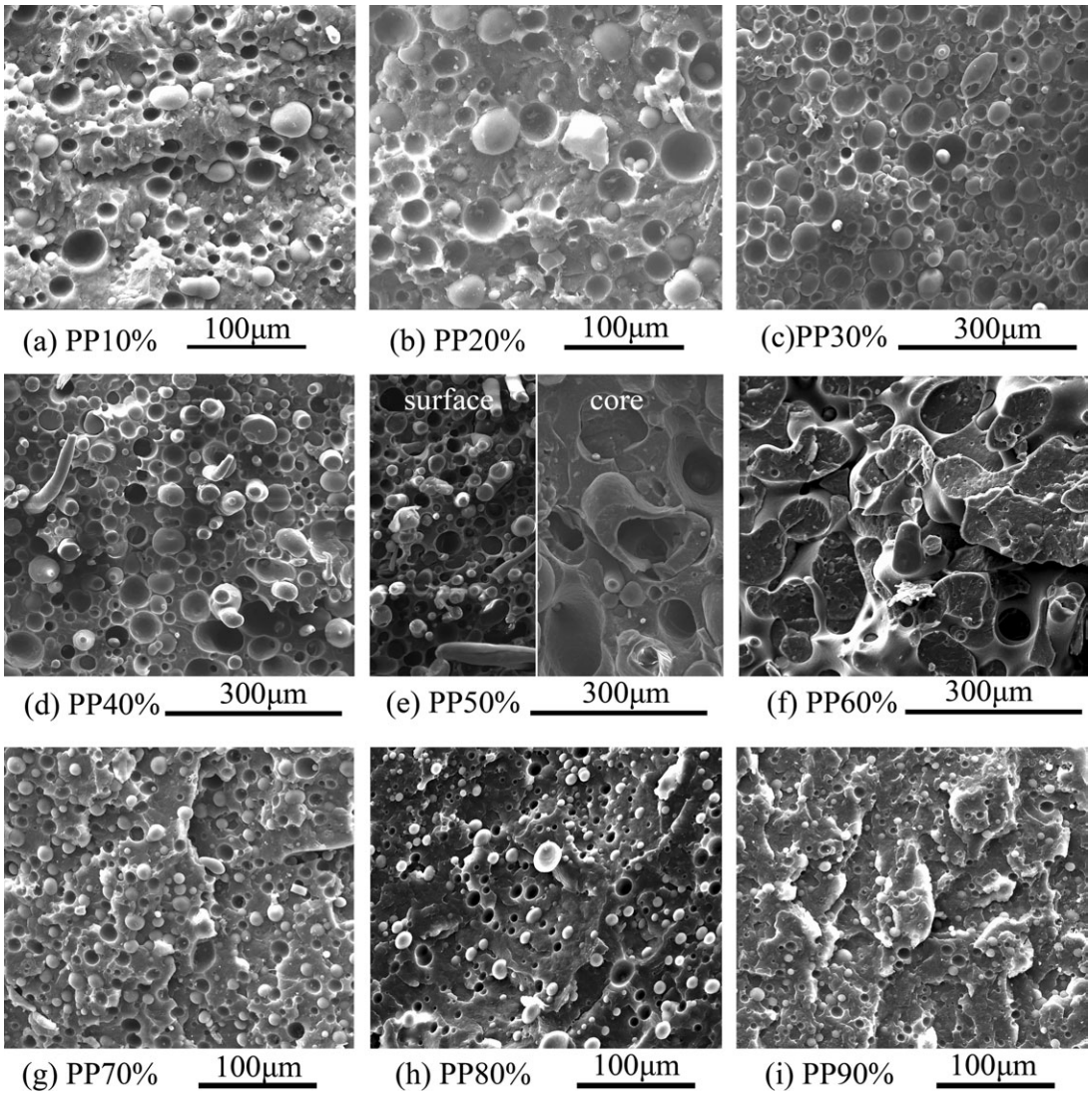

Figure 13. Morphology of PP/PA blends prepared by twin-screw extruder (vertical to the extrusion direction).

11th, and 12th VPCUs, respectively. From the 10th to 12th VPCU, the blends mix and homogenize further, which average diameters of droplets are 3.24, 2.41, and 2.02 μm, respectively.

The dynamical elongational deformation field generated by the vane extruder makes the striation thickness and the droplet size decrease rapidly, and the exponential stretching makes vane extruder effective in polymer blending. A schematic of morphology development along the length of vane extruder is illustrated in Figure 9.

Effect of Processing Method on the Morphology of Blends

Samples broken in perpendicular direction to the flow are used for observation. Figure 10 presents the morphologies of PP/PS blends prepared by vane extruder and twin-screw extruder, respectively. It can be seen that the droplet size of PP/PS blend prepared by the vane extruder are smaller than that prepared by twin-screw extruder. For comparison, the droplet diameter of PS dispersed phase is summarized in Figure 11. The average diameter of PP/PS blend droplet prepared by vane extruder is 0.75 μm, while that prepared by twin-screw extruder is 1.1 μm. Similarly, the droplet diameter distribution has the same trend, which for PP/PS blend of the vane extruder ranges from 0.3 to 1.9 μm, while that prepared by twin-screw extruder is from 0.2 to 4.7 μm. These indicate that the vane extruder has a much higher dispersive mixing efficiency than twin-screw extruder.

Morphologies of PP/PA blends with different content ratio prepared by vane extruder and twin-screw extruder are presented in Figures 12 and 13, respectively. It can be seen that no matter being prepared by vane extruder or twin-screw extruder, the effect of the content ratio on the morphologies of PP/PA blends is the same. When PP content is below 50%, the PP phase disperses in PA matrix are shown as droplet structure and the droplet size increases with increasing the loading of PP. Also noteworthy is that when PP content is up to 60%, the

Table II. Average Diameter (μm) of Droplets in Blends Prepared by Vane Extruder and Twin-Screw Extruder

Blends	PP/PA									PP/PS
Content ration	10/90	20/80	30/70	40/60	50/50	60/40	70/30	80/20	90/10	70/30
Vane extruder	6.21	7.18	9.30	10.38	12.80	-	6.45	3.85	3.64	0.75
Twin-screw extruder	10.69	14.12	18.59	19.51	20.27	-	8.40	5.38	4.88	1.10

morphologies of both PP and PA appear to be continuous. The phase reversion occurs at the content ratio of PP/PA of 70/30 and PA disperses in the PP matrix. As compared with Figures 12 and 13, it can be found that, at a given PP content, the droplet size of dispersed phase in PP/PA blends prepared by vane extruder is smaller than that prepared by twin-screw extruder. Furthermore, an interesting phenomenon is observed in PP/PA (50/50) blend. As shown in Figure 13(e), PP/PA (50/50) blend prepared by twin-screw extruder reveals smaller droplets in surface layer and larger droplet in core layer, while that prepared by vane extruder totally displays smaller droplets, indicating a much more uniform dispersed phase in blends of vane extrusion. One possible explanation for this phenomenon is that the shear stress acted on surface layer of blends is stronger than on core layer in twin-screw extruder, while blends in vane extruder suffer uniform elongational stress.

Shown in Table II is the average diameter of dispersed phase for PP/PA blends with different content ratio. The diameters of PP dispersed phase in blends prepared by vane extruder and twin-screw extruder range from 6.21 to 12.80 μm and 10.69 to 20.27 μm, respectively. Similarly, the PA droplets with size range of 3.64–6.45 μm and 4.88–8.40 μm exist in the blends prepared by vane extruder and twin-screw extruder, respectively. The data shows clearly that the droplet size of dispersed phase in PP/PA blends prepared by the vane extruder is smaller than that prepared by twin-screw extruder. Therefore, it is demonstrated that the vane extruder is more effective for processing immiscible polymer blends of PP/PA blends.

CONCLUSION

A novel vane extruder based on elongational deformation flow is designed to process polymeric materials, in which materials suffer from strong elongational deformation. PP/PS (70/30) blend is used to study the morphology development in the vane extruder. The result shows that the solid pellets of PP/PS blend are melted quickly in the first five VPCUs, indicating the strong melting ability and short melting length of the vane extruder. Besides, the blend is elongated in both circumferential and axial direction, and the strong elongational deformation field makes the dispersed phase change from stretched striations to droplets rapidly and mix uniformly finally.

PP/PA and PP/PS blends are used to compare the morphologies of blends prepared by the vane extruder and twin-screw extruder, respectively. The results reveal that the droplet size of dispersed phase in blends prepared by vane extruder is smaller than that prepared by twin-screw extruder, indicating vane extruder has better mixing ability than twin-screw extruder.

ACKNOWLEDGMENTS

The authors wish to acknowledge the National Nature Science Foundation of China (Grant 10872071, 50973035 and 50903033), the Fundamental Research Funds for the Central Universities (NO.2011ZM0063) and National Key Technology R&D Program of China (Grant 2009BAI84B05 and 2009BAI84B06) for the financial supports.

REFERENCES

1. Koning, C.; Vanduin, M.; Pagnoulle, C.; Jerome, R. *Prog. Polym. Sci.* **1998**, *23*, 707.
2. Debolt, M. A.; Robertson, R. E. *Polym. Eng. Sci.* **2006**, *46*, 385.
3. Potente, H.; Bastian, M.; Gehring, A.; Stephan, M.; Potschke, P. *J. Appl. Polym. Sci.* **2000**, *76*, 708.
4. Deyrail, Y.; Fulchiron, R.; Cassagnau, P. *Polymer* **2002**, *43*, 3311.
5. Ottino, J. M.; Chella, R. *Polym. Eng. Sci.* **1983**, *23*, 357.
6. Elmendorp, J. J. *Polym. Eng. Sci.* **1986**, *26*, 418.
7. Machado, A. V.; Duin, M. V.; Covas, J. A. *Polym. Eng. Sci.* **2002**, *42*, 2032.
8. Potente, H.; Bastian, M.; Bergemann, K.; Senge, M.; Scheel, G.; Winkelmann, T. *Polym. Eng. Sci.* **2001**, *41*, 222.
9. Wilczynski, K.; Tyszkiewicz, A.; Szymaniak, Z. *Mater. J. Process Technol.* **2001**,*109*, 320.
10. Jun, H. S.; Hwang, W. R.; Kwon, T. H. *Int. Polym. Proc.* **2004**, *20*, 218.
11. Lindt, J. T.; Ghosh, A. K. *Polym. Eng. Sci.* **1992**, 32, 1802.
12. Tyagi, S.; Ghosh, A. K. *Polym. Eng. Sci.* **2002**, *42*, 1309.
13. Huang, H. X.; Huang, Y. F.; Li, X. *J. Polym. Test.* **2007**, *26*, 770.
14. Sundararaj, U.; Macosko, C. W.; Rolando, R. J.; Chan, H. T. *Polym. Eng. Sci.* **1992**, 32, 1814.
15. Lee, J. K.; Han, C. D. *Polymer* **2000**, *41*, 1799.
16. Utracki, L. A.; Shi, Z. H. *Polym. Eng. Sci.* **1992**, 32, 1824.
17. Shi, Z. H.; Utracki, L. A. *Polym. Eng. Sci.* **1992**, 32, 1834.
18. Bordereau, V.; Carrega, M.; Shi, Z. H.; Utracki, L. A.; Sammut, P. *Polym. Eng. Sci.* **1992**, 32, 1846.
19. Huneault, M. A.; Shi, Z. H.; Utracki, L. A. *Polym. Eng. Sci.* **1995**, *35*, 115.
20. Bourry, D.; Favis, B. D. *Polymer* **1998**, 39, 1851.
21. Zumbrunnen, D. A.; Chhibber, C. *Polymer* **2002**, *43*, 3267.
22. Jana, S. C.; Sau, M. *Polymer* **2004**, *45*, 1665.
23. Stary, Z.; Machui, F.; Munstedt, H. *Polymer* **2010**, *51*, 3744.
24. DeRouseel, P.; Khakhar, D. V.; Ottino, J. M. *Chem. Eng. Sci.* **2001**, *56*, 5511.
25. DeRouseel, P.; Khakhar, D. V.; Ottino, J. M. *Chem. Eng. Sci.* **2001**, *56*, 5531.

26. Grace, H. P. Presented at Third Engineering Foundation of Research Conference on Mixing, Andover, NH, August 9–14, **1971**.
27. Ranwendaal, C.; Osswald, T.; Gramann, P. *Int. Polym. Proc.* **1999**, *14*, 28.
28. Suzaka, Y. U.S.Pat.4,334,783 (**1982**).
29. Bouquey, M.; Loux, C.; Muller, R.; Bouchet, G. *J. Appl. Polym. Sci.* **2011**, *119*, 482.
30. Novais, R. M.; Covas, J. A.; Paiva, M. C. *Compos. Part A Appl. Sci.* **2012**, *43*, 833.
31. Qu, J. P. Can. Pat.CN200810026054X (**2009**).
32. Qu, J. P.; Zhang, G. Z.; Chen, H. Z.; Yin, X. C.; He, H. Z. *Polym. Eng. Sci.* **2012**, DOI: 10.1002/pen.23176.
33. Qu, J. P.; Liu, L. M.; Tan, B.; Liu, S. R.; Chen, H. X.; Feng, Y. H. *Polym. Compos.* **2012**, *33*, 185.
34. Molden, G. F. *J. Mater. Sci.* **1969**, *4*, 283.